

## Thermal and chemical evidence for rapid water exchange across the sediment–water interface by bioirrigation in the Indian River Lagoon, Florida

*Jonathan B. Martin*<sup>1</sup>

Department of Geological Sciences, 241 Williamson Hall, University of Florida, Gainesville, Florida 32611-2120

*Jaye E. Cable*

Department of Oceanography and Coastal Sciences, Coastal Ecology Institute, Louisiana State University, 208 Old Coastal Studies Bldg., Baton Rouge, Louisiana 70803

*John Jaeger*

Department of Geological Sciences, 241 Williamson Hall, University of Florida, Gainesville, Florida 32611-2120

*Kevin Hartl*

Department of Geological Sciences, 241 Williamson Hall, University of Florida, Gainesville, Florida 32611-2120

*Christopher G. Smith*

Department of Oceanography and Coastal Sciences, Coastal Ecology Institute, Louisiana State University, 208 Old Coastal Studies Bldg., Baton Rouge, Louisiana 70803

### *Abstract*

Time-series measurements of chloride (Cl<sup>-</sup>) concentrations in lagoon and pore waters of an estuary on the east coast of Florida (Indian River Lagoon) demonstrate exchange of lagoon surface water to depths of ~40 cm in the sediment in less than 46 h. The exchange rate may be as fast as 150 cm d<sup>-1</sup> based on models of the decay in the amplitude of diurnal temperature variations and the time lag of maxima and minima of the temperature variations at depths of 15 and 30 cm below the sediment–water interface. These flow rates indicate a minimum residence time of 0.33 d for the pore water. Considering the small tides and waves, rate of the exchange, and large number of bioturbating organisms in the Indian River Lagoon, the exchange of water is driven largely by bioirrigation. The exchange provides a greater flux of excess radon-222 from the sediment to the lagoon than would occur from diffusion alone. The exchange also pumps oxygenated water into the sediments, thereby enhancing organic carbon remineralization and the flux of nitrogen from sediments to the lagoon water. High rates of exchange across the sediment–water interface indicate that marine sources are volumetrically more important than terrestrial sources to submarine groundwater discharge in the permeable sediments of this estuary.

Conceptualization of submarine groundwater discharge (SGD) has long been based on the Dupuit–Ghyben–Herzberg model of a buoyant freshwater lens that overlies seawater and discharges at a seepage face along the shoreline (Cooper 1959). This conceptualization predicts that SGD represents a flow path from continents to the oceans for water and dissolved components. Direct measurements of SGD using tools such as seepage meters (Lee 1977) and radioisotope tracers (Cable et al. 1996a; Burnett et al. 2003) have found that more water may discharge than is available to recharge the regional terrestrial aquifers, for example, compare Moore (1996) and Li et al. (1999). This observation indicates that SGD is composed of both terrestrial and marine sources of water

and has led to the definition of total SGD as all water flowing from the sediment to the overlying water regardless of its origin (Taniguchi et al. 2002; Burnett et al. 2003). Because the terrestrial source is limited by recharge on the continents, but the marine source is essentially unlimited, the magnitude of total SGD depends on those processes allowing marine water to enter coastal aquifers and bottom sediments. This paper focuses on those processes, their rates and controls, and consequences of this exchange for chemical fluxes to estuarine water.

Chemical fluxes will depend on the relative magnitudes of marine and terrestrial sources of the exchanging water because of differences in their chemical composition. The terrestrial fraction of SGD will have salinities distinct from marine sources, and thus affect benthic ecosystems in marine systems (Miller and Ullman 2004). The terrestrial fraction also could carry contaminants from terrestrial to marine systems, with nutrients being the most widely studied component. On the other hand, the marine fraction should have salinities and bulk chemical compositions similar to the overlying water except for those solutes altered during diagenetic reactions with aquifer rocks and

<sup>1</sup> Corresponding author (jbmartin@ufl.edu).

### *Acknowledgments*

We thank two anonymous reviewers for their thoughtful and thorough reviews, which have greatly improved this paper.

Support for the project was provided by the St. Johns River Water Management District through contract SG458A and the National Science Foundation through grant EAR-0403461.

bottom sediments. Consequently, only fluxes of reactive solutes will be important from marine sources of water.

A variety of processes have been identified that could incorporate seawater into SGD. Seawater is entrained in freshwater SGD through dispersive mixing across the freshwater–saltwater boundary in the subsurface (Cooper 1959; Li and Jiao 2003). Seawater also is exchanged across the sediment–water interface through processes such as wave and tidal pumping (Shum 1993; Li et al. 1999), density mixing (Bokuniewicz et al. 2004; Moore and Wilson 2005), variations in the terrestrial water table level (Michael et al. 2005), and irrigation by bioturbating organisms, commonly referred to as bioirrigation (Aller 1980; Boudreau and Marinelli 1994; Schluter et al. 2000). Physical processes driving exchange, such as wave and tidal pumping, have been replicated and studied in laboratory experiments (Huettel and Webster 2001). In natural settings, exchange has been observed as variations through time in concentrations of chemical tracers in pore waters (Schluter et al. 2000; Cable et al. 2004; Martin et al. 2004). The exchange rate is poorly quantified because time variations of the chemical composition of the surface water, which controls pore water composition, occur more slowly than the exchange rate (Martin et al. 2004). The exchange rate is critical to estimates of solute fluxes associated with SGD.

In this paper, we use chemical and thermal observations to show that SGD in the Indian River Lagoon, Florida, is composed primarily of estuarine surface water exchanging across the sediment–water interface. We present a technique utilizing time-series variations in temperature at different depths in the sediment to estimate the rate of exchange. Based on characteristics of the lagoon, we suggest the primary driving force for exchange is bioirrigation, although density variations will affect the flow. The chemical composition of water exchanged across the sediment–water interface appears to be modified by radioactive decay of radium-226 ( $^{226}\text{Ra}$ ) and remineralization of organic matter, and as a result we suggest the exchange is an important for chemical cycling in the lagoon.

### Sampling location and methods

To determine the magnitude of marine SGD, we sampled the water column and pore water to depths as great as 230 cm below the seafloor (cmbsf) throughout the northern half of the Indian River and Banana River lagoons on the Atlantic coast of Florida. The Indian River lagoon system, which is composed of the Indian River, Banana River, and Mosquito lagoons (Fig. 1), has an average depth of  $\sim 1$  m, a maximum width of  $\sim 7$  km, and extends for more than 250 km along the coast. The lagoon system is connected to the Atlantic Ocean by three inlets that are all located in the southern half of the system, thus limiting exchange with the ocean (Smith 1993). The region receives  $\sim 150$  cm of precipitation per year and approximately half occurs during the 4-month rainy season between June and September. The restricted exchange with the ocean, combined with seasonal variations in pre-

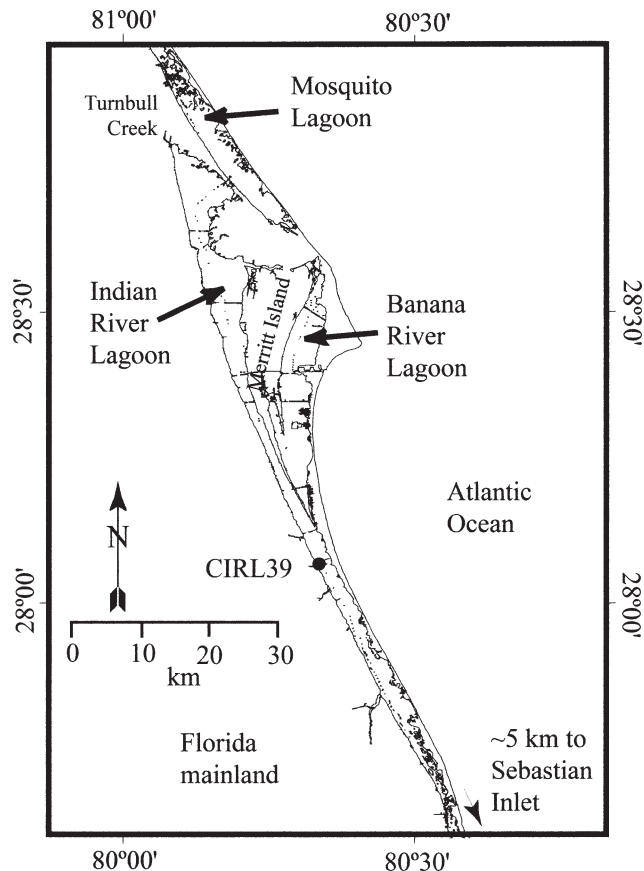


Fig. 1. Location map of the Indian River Lagoon system including the southern portion of Mosquito Lagoon, Banana River Lagoon, and the northern portion of Indian River Lagoon. Map shows location of sampling station CIRL39.

cipitation and evaporation rates, leads to wide fluctuations of salinity of the lagoon water column, thus providing a robust tracer of exchange across the sediment–water interface (Martin et al. 2004).

During the project, five stations were sampled throughout the field area for a period of 1 year (May 2003 to May 2004). Because temporal variations in compositions are similar for pore water from all stations, only one station (CIRL39:  $28^{\circ}06'59.7''\text{N}$ ,  $80^{\circ}37'05.2''\text{W}$ ) is described here as a representative example. In addition, comparative thermal data were collected at this station during the final sampling in May 2004. CIRL39 is located  $\sim 500$  m from the western margin of the lagoon and seaward of the aquifer seepage face, which is restricted to  $\sim 25$  m from the shoreline at this location (Martin et al. 2005a).

Samples of pore water and surface water were collected approximately monthly between 12 May and 26 September 2003, on 28 September 2003, and on 06 February and 27 May 2004. Pore water was extracted from the sediment using a peristaltic pump attached to a multilevel piezometer [“multisampler” (Martin et al. 2003)], which was installed at the beginning of the project and remained in the sediment throughout the year. During sampling, the water was measured for temperature, conductivity, salinity, and dissolved oxygen. Samples were collected following stabi-

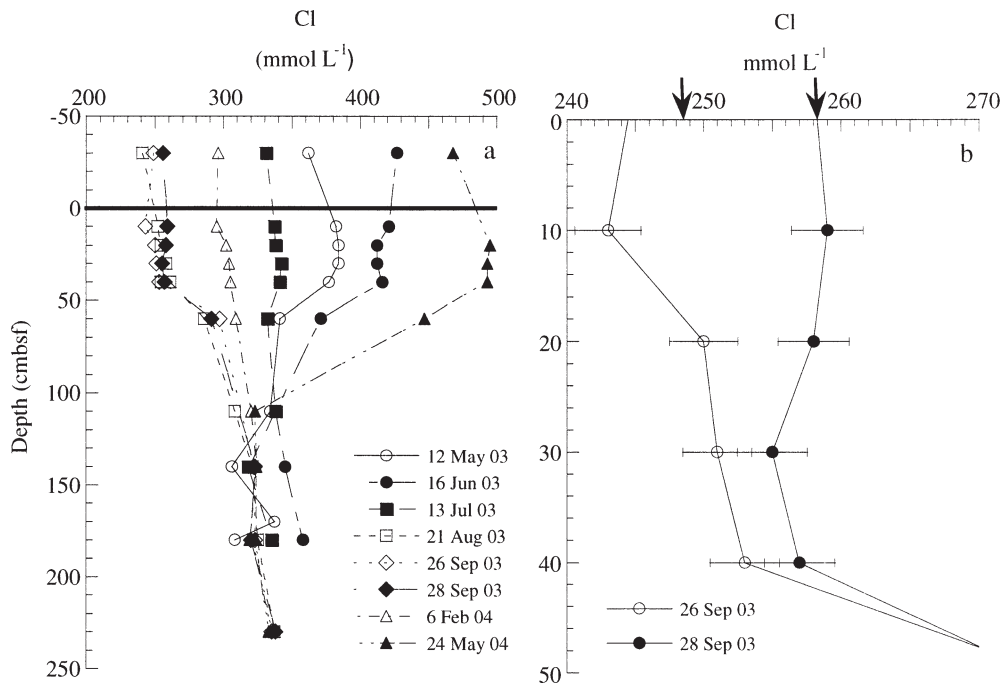


Fig. 2. Pore water  $\text{Cl}^-$  concentrations. (a)  $\text{Cl}^-$  concentrations versus depth in the sediment and in the water column for various times during the year. The solid line at 0 cmbsf represents the sediment–water interface. (b)  $\text{Cl}^-$  concentrations versus depth for samples collected 46 h apart. Note the difference in both the depth and concentration scales between plots (a) and (b). The arrows in (b) indicate the  $\text{Cl}^-$  concentration in the water column. Error bars represent  $\pm 1\%$  of the value.

lization of all parameters, which usually occurred within a few minutes after pumping began. In the laboratory, samples were titrated with silver nitrate ( $\text{AgNO}_3$ ) to determine  $\text{Cl}^-$  concentration (Fig. 2). Precision was estimated to be  $\sim 1\%$  through repeated measurements of an internal seawater standard. Separate aliquots of the water were preserved in triplicate for total  $^{222}\text{Rn}$  analysis by injecting 10  $\text{cm}^3$  of water into glass scintillation vials prefilled with 10 mL of high efficiency mineral oil. Radon-222 activities were measured using a Packard Tri-Carb 3100TR liquid scintillation counter. The  $^{226}\text{Ra}$  activities were measured by cryogenically extracting  $^{222}\text{Rn}$  in secular equilibrium with the  $^{226}\text{Ra}$  and counting the  $^{222}\text{Rn}$  with alpha scintillation counters. Excess  $^{222}\text{Rn}$  was calculated by subtracting  $^{226}\text{Ra}$  from total  $^{222}\text{Rn}$  activities and decay-correcting back to the time of sampling (Fig. 3).

Seepage rates were measured with manual Lee-type seepage meters (Lee 1977) during the sampling trips on 12 May, 18 June, 13 July, 26 September 2003, and 25 May 2004. Seepage meters were deployed in duplicate at the start of the project and remained in place throughout the year. Seepage rates had been measured at CIRL39 three times prior to this project in May, August, and December 2000. The average rate of all 13 measurements is  $7.1 \text{ cm d}^{-1}$  with a standard deviation of  $1.9 \text{ cm d}^{-1}$  (Fig. 4).

Temperature was measured in the water column and 15 and 30 cmbsf using automatic logging waterproof thermistors (Onset Optic Stowaway temperature loggers) at 1-min

intervals between 18:00 h on 23 May 2004 and 12:18 h on 27 May 2004. The thermistors were hung by a thin nylon string in a 3.175-cm (inside diameter) PVC pipe that had been driven into the sediment several months prior to sampling. The pipe was filled with ambient water and allowed to equilibrate prior to being used. After the thermistors were installed in the pipe, it was capped to prevent exchange of water from the surface to the interior of the pipe. The thermistors have an accuracy of  $0.2^\circ\text{C}$  resulting in step changes in measured temperatures, which were smoothed by averaging over a 0.5-h window (Fig. 5).

Two types of cores were collected from the site, and the bottom sediment was surveyed for types of burrow structures. Five  $\sim 3$ -m sediment vibrocores were collected around the sampling site to determine porosity and spatial variability of the sediment characteristics. One core was collected within a few meters of where temperature and water were sampled, and four other cores were collected 100 m north, south, east, and west of the sampling site. Bulk density of the cores was measured with a Geotek Multi-sensor Core Logger and converted to porosity assuming two end-member mixing between pore water with density of  $1.023 \text{ g cm}^{-3}$  and solid with a density of  $2.65 \text{ g cm}^{-3}$ . There was little heterogeneity in porosity among the five cores. Three polycarbonate x-ray slab cores were also collected at the edges of a 1 m by 1 m quadrat. The slab cores measured 20 cm wide by 2 cm thick by 50 cm long and were x-rayed in the laboratory to observe burrow densities (Fig. 6). A quantitative inventory of active

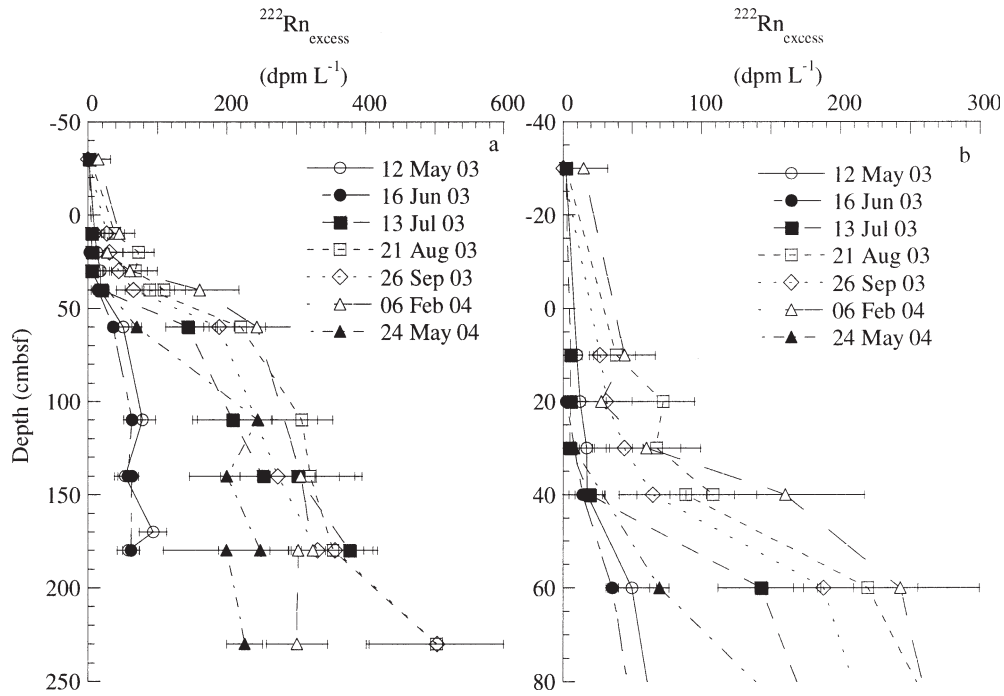


Fig. 3. Pore water  $^{222}\text{Rn}_{\text{excess}}$  activities versus depth. (a)  $^{222}\text{Rn}_{\text{excess}}$  activities over the total depth sampled at CIRL39. (b)  $^{222}\text{Rn}_{\text{excess}}$  activities over the upper 80 cm of the depth sampled. Note the difference in both the depth and activity scales between plots (a) and (b). Error bars represent the standard deviation of the triplicate measurements.

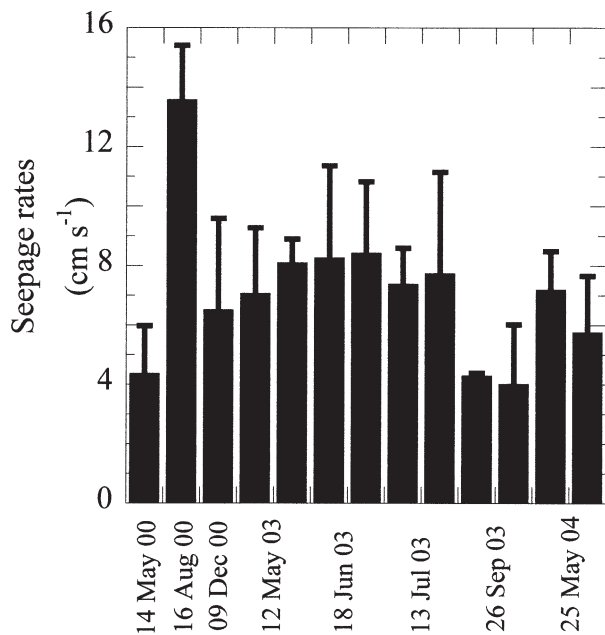


Fig. 4. Histogram of seepage rates measured three times during 2000 and five times between May 2003 and May 2004. The seepage rates were measured in duplicate from two different seepage meters for each sampling time in 2003 and 2004.

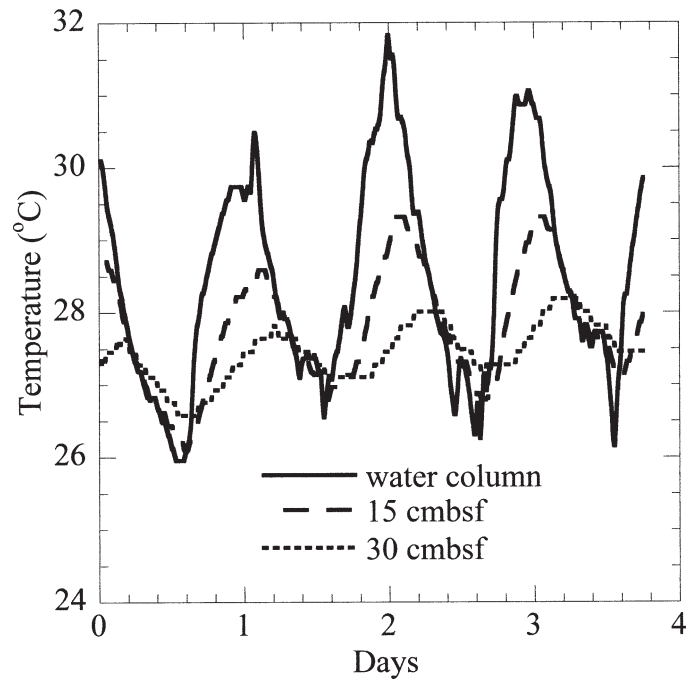


Fig. 5. Temperature variations in the water column, 15 cmbsf, and 30 cmbsf. The temperature data were logged at 1-min intervals between 18:00 h on 23 May 2004 and 12:18 h on 27 May 2004. The data have been smoothed using a 0.5-h running average.

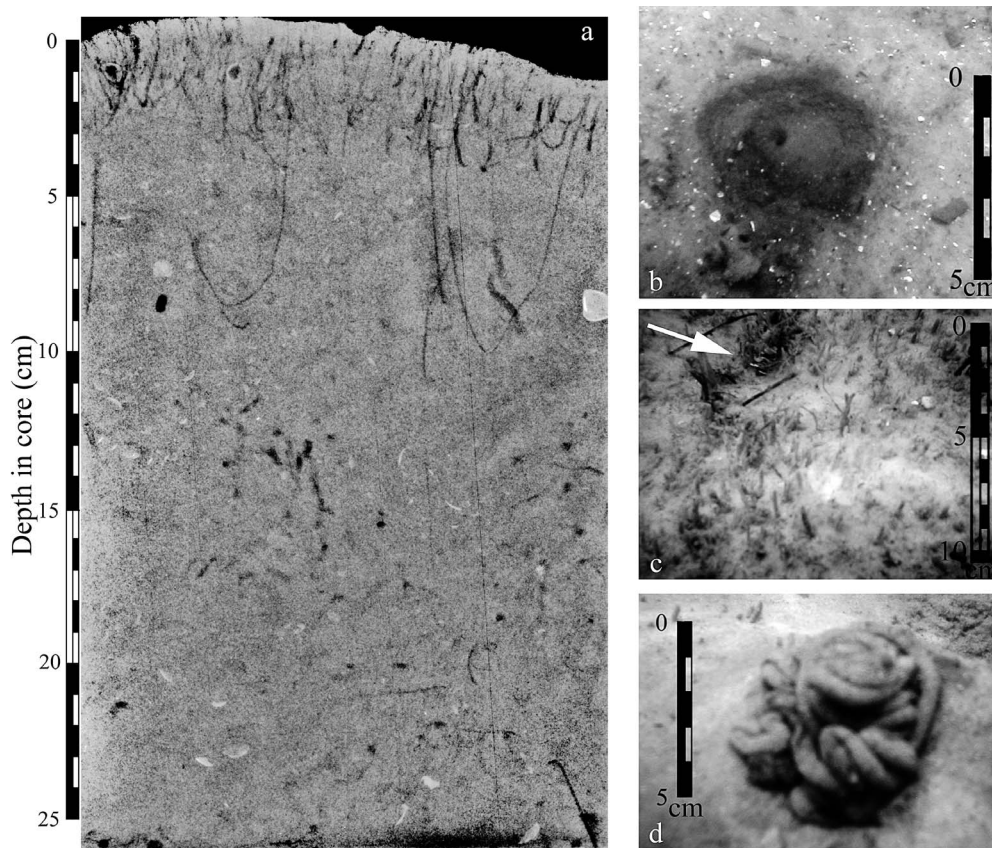


Fig. 6. (a) X-ray radiograph negatives (denser = lighter) of slab cores from May 2004 CIRL39. Fine burrows in the upper 5 cm are likely made by amphipods, and the small open holes near the bottom of core likely made by *Diopatra*. Photographs of bottom sediment at CIRL39 showing representative burrows and surface traces of (b) *Callianassa* sp., (c) *Diopatra* sp. (indicated by an arrow) with amphipods in the foreground, and (d) *Arenicola crisata*.

(i.e., evidence of recent burrowing) biogenic structures was taken of the surface sediment within the quadrat to enumerate structure densities. These data are reported in Martin et al. (2005b) and Cable et al. (unpubl. data). The quadrat was randomly placed on the sediment surface along a shore-parallel, constant-water depth ( $\sim 1$  m) transect with a total of five counts made north and south, respectively, of the main sampling area.

Sediments from the piston cores were used in slurry measurements of  $^{226}\text{Ra}$  activities. These experiments involved mixing known weights of sediment with water in closed vessels and agitating the sediment-water slurry mixture to allow escape into the headspace of  $^{222}\text{Rn}$  produced from the decay of sedimentary  $^{226}\text{Ra}$ . The slurry was agitated for sufficient time to allow  $^{222}\text{Rn}$  to come into secular equilibrium with  $^{226}\text{Ra}$  in the sediment. This procedure generates a maximum possible value for  $^{222}\text{Rn}$  contributed to pore waters from sedimentary  $^{226}\text{Ra}$  because some  $^{222}\text{Rn}$  in the natural setting may remain trapped in the sediment.

## Results

*Time series chemical variations*—In the water column, variations of up to a factor of 2 in  $\text{Cl}^-$  concentrations occur

over the year, and these variations propagate into the sediment (Fig. 2). Variations of  $\text{Cl}^-$  concentrations in the pore water reflect two water masses: one above 40 cmbsf and the other below  $\sim 150$  cmbsf, with the two water masses separated by steep gradients. The lower water mass has  $\text{Cl}^-$  concentrations that are more constant through time than those in the upper water column, with an average value of  $\sim 329$   $\text{mmol L}^{-1}$ . This concentration is identical within error to the average value of eight samples collected during the year from the water column ( $330$   $\text{mmol L}^{-1}$ ), indicating there is little contribution of freshwater from terrestrial sources. It is unlikely that terrestrial sources contribute to SGD at this location because the seepage face is located  $\sim 500$  m closer to the shore than the sampling site (Martin et al. 2005b). The  $\text{Cl}^-$  concentrations of the lower water mass vary by less than 10% through time, with a range of 318 to 354  $\text{mmol L}^{-1}$ . This variation indicates the lower water mass may also exchange with the upper water mass but over longer time scales than in the upper water mass.

In the upper water mass,  $\text{Cl}^-$  concentrations are constant with depth at any one sampling time and are similar to concentrations in the water column, which ranges from  $\sim 250$   $\text{mmol L}^{-1}$  on 28 September 2003 near the end of the wet season to  $\sim 495$   $\text{mmol L}^{-1}$  on 24 May 2004 near

Table 1. Measured and modeled temperature amplitudes and time lags.

Water column Date	24 May 04		25 May 04		26 May 04		27 May 04
Maximum or minimum values	Min.	Max.	Min.	Max.	Min.	Max.	Min.
Time*	6:40	19:46	7:08	17:51	9:00	17:04	7:10
Temp. (°C)	25.96	30.49	26.55	31.83	26.26	31.06	26.10
Measured amplitude (°C)		4.53	3.94	5.28	5.57	4.80	4.96
		15 cmbsf					
Time*	8:18	20:23	7:50	19:06	9:13	18:42	7:47
Temp. (°C)	26.09	28.59	26.79	29.32	26.79	29.32	27.09
Measured amplitude (°C)		2.50	1.80	2.53	2.53	2.53	2.23
Modeled amplitude (°C)†		0.8	0.7	1.0	1.0	0.9	0.9
% difference‡		33	40	38	40	34	40
Measured time lag (h)§	1.6	0.6	0.7	1.2	0.2	1.6	0.6
		30 cmbsf					
Time*	8:37	22:50	7:27	22:18	9:24	21:00	7:26
Temp. (°C)	26.55	27.82	27.11	28.01	27.11	28.19	27.46
Measured amplitude (°C)		1.27	0.71	0.90	0.90	1.08	0.73
Modeled amplitude (°C)†		0.2	0.1	0.2	0.2	0.2	0.2
% difference‡		12	18	19	20	15	22
Measured time lag (h)	1.9	3.1	0.3	4.5	10.4	3.9	0.3

\* Time when the maximum or minimum temperature was reach (Fig. 2).

† Amplitudes calculated using Eq. 3.

‡ Percentage difference between the measured and modeled temperature amplitude.

§ Difference between time when maximum or minimum temperature was reached in the water column and at depth in the sediment.

the end of the dry season. These profiles reflect complete exchange of pore water with overlying lagoon water to depths in the sediment between 40 and 60 cmbsf from one sampling time to the next. With an effective diffusion coefficient of  $\sim 4.6 \times 10^{-6} \text{ cm}^2 \text{ s}^{-1}$ , the replacement is too rapid to result from diffusive exchange of  $\text{Cl}^-$  (Martin et al. 2004), indicating that advection is the primary transport process for the  $\text{Cl}^-$ .

Changes of pore water  $\text{Cl}^-$  concentrations were measured over a 2-d period between 26 September and 28 September 2003, when  $\text{Cl}^-$  concentrations in the water column increased from  $249 \text{ mmol L}^{-1}$  to  $256 \text{ mmol L}^{-1}$ . The change in water-column composition is reflected in the pore water to depths of  $\sim 40$  cmbsf (Fig. 2b), indicating that the pore water was replaced with surface water over this time. For water to reach depths of 40 cm in the sediment in 2 d, the average rate of flow would have to be at least  $20 \text{ cm d}^{-1}$ , and these flow rates could be higher if the exchange occurred in less than the 46 h separating the two sampling events. Determining flow rates faster than those observed here requires use of a tracer that varies more rapidly than the  $\text{Cl}^-$  concentration of the lagoon water. Nonetheless, these observations demonstrate pore-water exchanges with overlying surface water at a rate at least as rapid as the change in the  $\text{Cl}^-$  concentration of the lagoon water.

The profiles of  $^{222}\text{Rn}_{\text{excess}}$  activity show steadily increasing  $^{222}\text{Rn}_{\text{excess}}$  activities with depth in the sediment at all sampling times (Fig. 3). These profiles can differ from those of  $\text{Cl}^-$  concentrations because unlike  $\text{Cl}^-$ , which is conservative, sediment-bound  $^{226}\text{Ra}$  can provide a source of  $^{222}\text{Rn}$  to the pore waters. Even in the upper water mass as defined by constant  $\text{Cl}^-$  concentrations, only the

uppermost sample in the pore water has  $^{222}\text{Rn}_{\text{excess}}$  activity similar to the  $^{222}\text{Rn}_{\text{excess}}$  activity in the water column (Fig. 3b). All  $^{222}\text{Rn}_{\text{excess}}$  profiles also display a strong inflection at a depth of around 40 cmbsf, indicating that they are not controlled solely by diffusion of  $^{222}\text{Rn}$  from a source deep in the sediment; exchange between the lagoon water and pore waters will also influence the  $^{222}\text{Rn}_{\text{excess}}$  profiles.

*Temperature variations*—Changes in water temperature can occur more rapidly than changes in the chemical composition of water and thus may be used to estimate the rate at which heat is carried into the sediment by water exchange. Recent thermal observations on the Carolina continental shelf have been used to make inferences about rates of discharge of terrestrial SGD and the effects of storm setup and wave pumping on the SGD (Moore and Wilson 2005). We take a different approach here and use observations of variation in temperature in the sediment to constrain models of conduction of heat into the sediment (Carslaw and Jaeger 1959).

At CIRL39, the water column temperature fluctuates diurnally by as much as  $5.6^\circ\text{C}$ , and these fluctuations, which have identical frequency but smaller amplitudes, are reflected in pore-water temperature at depths of 15 and 30 cmbsf (Fig. 5). The amplitudes of the diurnal variations decrease to as little as  $1.8^\circ\text{C}$  at 15 cmbsf and  $0.7^\circ\text{C}$  at 30 cmbsf (Table 1). In addition to the decrease in the temperature amplitude, the pore water temperature minima and maxima increasingly lag the water column minima and maxima with increasing depth in the sediment. The decrease in the amplitude and the lag of the temperature minima and maxima reflect the movement of heat by

conduction and convection into the sediment from the surface.

Assuming heat transfer by conduction, observed variations in temperature with depth can be modeled using a differential equation of the form

$$\frac{\partial^2 T}{\partial z^2} - \frac{1}{\kappa} \frac{\partial T}{\partial t} = 0 \quad (1)$$

where  $T$  represents temperature,  $z$  represents depth into the sediment (positive downward),  $\kappa$  represents the thermal diffusivity, and  $t$  represents time. For a boundary condition where surface temperatures fluctuate as a harmonic function of time, e.g.,  $T = A \cos(\omega t)$ , where  $A$  is the amplitude of the variation and  $\omega$  is angular velocity  $2\pi/t_0$ , with a periodicity of  $t_0 = 24$  h, the analytical solution to Eq. 1 is (Carslaw and Jaeger 1959)

$$T = Ae^{-kz} \cos(\omega t - kz), \quad (2)$$

where

$$k = \sqrt{\omega/2\kappa}.$$

At a given depth  $z$  in the sediment, the amplitude,  $A_z$ , of the harmonic oscillation of the temperature is:

$$A_z = A \exp\left[-z(\pi/t_0\kappa)^{1/2}\right] \quad (3)$$

and the time lag  $t_L$  for the propagation of the heat to depth  $L$  is:

$$t_L = z\sqrt{t_0/4\pi\kappa} \quad (4)$$

We have used Eq. 3 to calculate the amplitude of diurnal temperature variations at 15 and 30 cmbsf that would be expected from the measured amplitudes of the changes in temperature of the water column, assuming  $\kappa = 2.6$  to  $2.8 \times 10^{-3} \text{ cm}^2 \text{ s}^{-1}$  (Louden and Wright 2000). The measured amplitudes are 60–77% greater at 15 cmbsf and 78–88% greater at 30 cmbsf than modeled conductive values (Table 1). These differences suggest more heat is transferred to these depths than by conduction alone and exchange of water across the sediment–water interface may also transport heat into the sediments. Sunlight weakly illuminates the bottom of the lagoon at this station, suggesting that radiant heat could elevate the temperature of the surface sediment and influence this calculation. We have no measurements of increases in the temperature of the sediment surface from radiant heat but expect it to be small because only a limited amount of light penetrates through the  $\sim 1$  m water column to the bottom of the lagoon.

Equation 4 predicts that conduction to 15 and 30 cmbsf would take 6.5 and 13.1 h, respectively. At both depths, the measured time lags vary (Table 1) because of broad maxima and minima caused by limited resolution of the thermistors (Fig. 5). All measured time lags are shorter than predicted despite the variability, and similar to the

change in amplitudes; the shorter time lag may be explained by exchange of water across the sediment–water interface transferring heat more rapidly than by conduction alone. The averages of all measured time lags are 0.93 and 2.06 h at 15 and 30 cmbsf, respectively. Assuming the measured time lags reflect convection, specific discharge would be on the order of  $150 \text{ cm d}^{-1}$ , and suggests that the pore water has a residence time in the upper 50 cm of the sediment of  $\sim 0.33$  days.

## Discussion

In the following discussion, we use the observed chemical and temperature changes to estimate rates and volumes of water exchanged across the sediment–water interface and discuss potential causes of this exchange and its influence on chemical fluxes. Water flux will depend on sediment porosity, which averages  $45\% \pm 2\%$  ( $2\sigma$ ) with a range from 41–50%. If pore water has a residence time of 0.33 days based on thermal observations (Table 1),  $\sim 1.3 \text{ m}^3 \text{ m}^{-2} \text{ d}^{-1}$  of water is exchanged in the upper 50 cm of sediment. If the exchange requires 2 d as estimated by the changes in  $\text{Cl}^-$  concentrations (Fig. 2), then  $\sim 0.2 \text{ m}^3 \text{ m}^{-2} \text{ d}^{-1}$  would be exchanged.

The average of 13 separate seepage meter measurements yielded rates of  $7.1 \text{ cm d}^{-1}$  for net movement of water from the sediment, which equates to  $\sim 0.07 \text{ m}^3 \text{ m}^{-2} \text{ d}^{-1}$  (Fig. 4). This estimate is 3 times lower than the rate estimated here on the basis of changes in  $\text{Cl}^-$  concentrations and 19 times lower than the rate estimated on the basis of changes in temperature of the pore waters. All seepage meter measurements show only flow from the sediment to the water column even though processes likely responsible for driving exchange across the sediment–water interface (e.g., tidal pumping, wave pumping, seasonal variations of the water table, or bioirrigation) should cause flow both into and out of the sediment. Although some of the outflow may result from artifacts inherent in the seepage meter design (e.g., Shinn et al. 2002; Cable et al. unpubl. data), we use the seepage meter measurements as a qualitative measure of seepage rates and water exchange across the sediment–water interface to compare with other estimates of exchange.

*Possible mechanisms driving exchange*—In the Indian River Lagoon, it is unlikely that density differences (Bokuniewicz et al. 2004; Moore and Wilson 2005), tidal and wave pumping (Shum 1993; Huettel and Webster 2001), or seasonal variations in terrestrial water table (Michael et al. 2005) drive the exchange of water across the sediment–water interface. The small tidal range of  $\sim 10$  cm (Smith 1993), would be insufficient to drive water to depths as great as 40 cmbsf in the sediment in these moderately permeable ( $k_i \approx 1 \times 10^{-7} \text{ cm}^2$ ) muddy sands (Hartl et al. unpubl.). Furthermore, if exchange is as rapid as estimated from temperature variations, then tidal periodicity and seasonal variations of the water table are longer than the exchange time and would not drive exchange at the observed rate. Wave heights in the lagoon are limited by the small fetch across the lagoon, and bedforms are

typically only a few centimeters high, limiting Bernoulli pumping of water into the sediment (Shum 1993; Huettel and Webster 2001).

Density inversions have been shown to be a critical factor in the mixing of water across the sediment–water interface at the Carolina shelf, where density instability from decreasing salinity with depth in the sediment initiates convective mixing (Moore and Wilson 2005). Density differences cannot explain the exchange shown by variations in  $\text{Cl}^-$  concentrations (Fig. 2) because the lagoon and pore water are density stratified during most sampling times. For example, during the summer months salinity decreases and temperature increases, thereby lowering density of the water column from  $1,012.7 \text{ kg m}^{-3}$  on 18 June 2003 to  $1,007.7 \text{ kg m}^{-3}$  on 13 July 2003 to  $1,005.7 \text{ kg m}^{-3}$  on 21 August 2003 (calculated using IOC UNESCO equation of state: [HTTP://ioc.unesco.org/oceanteacher/resourcekit/M3/Converters/SeaWaterEquationOfState/Sea%20Water%20Equation%20of%20of%20of%20State%20Calculatorl.htm](http://ioc.unesco.org/oceanteacher/resourcekit/M3/Converters/SeaWaterEquationOfState/Sea%20Water%20Equation%20of%20of%20of%20State%20Calculatorl.htm)). Simultaneous with the drop in density in the water column, pore-water density at 60 cmbsf decreases from  $1,010.5$  to  $1,008.3$  to  $1,006.7 \text{ kg m}^{-3}$ . These data demonstrate that in July and August the lagoon and pore waters are density stratified, and in June insufficient density contrast is present to initiate convection even though the  $\text{Cl}^-$  concentrations reflect extensive exchange (Fig. 2). During the dry winter months, when salinity increases and temperature decreases in the lagoon water, density instabilities can occur, but calculations of the lagoon and pore water densities on 25 May 2004, during the most saline sampling time (Fig. 2), show that water density increases from the lagoon water ( $\rho = 1,021.5 \text{ kg m}^{-3}$ ) into the pore waters to a depth of 40 cmbsf ( $\sigma = 1,022.0 \text{ kg m}^{-3}$ ). A density inversion does not occur until salinities decrease rapidly between 40 and 60 cmbsf. Based on calculations necessary to initiate convections described by Moore and Wilson (2005), this density contrast is insufficient to initiate convection.

Bioirrigation is a commonly recognized phenomenon in marine sediments (Aller 1980; Boudreau and Marinelli 1994; Schluter et al. 2000), and all of the observed sediments in the lagoon are highly bioturbated, with active traces, burrows, and tubes made by thalassinidean shrimp (e.g., *Callianassa sp.* and/or *Upogebia affinis*), worms (*Arenicola cristata* and *Diopatra cuprea*), and smaller unidentified polychaete worms and burrowing amphipods (e.g., Fig. 6). The high density of bioirrigation organisms (Martin et al. 2005a; Cable et al. unpubl. data) suggests that bioirrigation may be an important process influencing the exchange. Rates of bioirrigation by burrowing shrimp have been found (*Callianassa sp.* and/or *Upogebia affinis*) to be up to  $7.2 \text{ L d}^{-1}$  (Forster and Graf 1995; Webb and Eyre 2004) and for worms (*Arenicola* and *Diopatra*) to be up to  $2.3 \text{ L d}^{-1}$  for individual burrows (Dales et al. 1970; Riisgard et al. 1996; Timmermann et al. 2002). Although a biological assessment of the quantity and distribution of burrowing organisms has not been completed at CIRL39, extensive evidence for the presence of these organisms has been found during surveys of the lagoon bottom (Fig. 6). A comparison of the estimated density of bioirrigating

organisms and published bioirrigation rates indicates the exchange rate could be  $\sim 0.05 \text{ m}^3 \text{ m}^{-2} \text{ d}^{-1}$  (Martin et al. 2005a; Cable et al. unpubl. data), which converts to a linear velocity of  $\sim 5 \text{ cm d}^{-1}$ . These values are close to the seepage rates measured by seepage meters of  $\sim 7 \text{ cm d}^{-1}$ .

Some burrowing organisms, such as thalassinidean shrimp, build structures with multiple entrances to the sediment (Forster and Graf 1995; Webb and Eyre 2004). The head space under seepage meters typically becomes strongly reducing with an associated increase in toxic compounds, including sulfide. If seepage meters cover only some of the entrances to the structure, the organisms may pump water through their burrow nests into the seepage meters to prevent contamination of their burrows, and thus contribute to the net outflow observed here and commonly in other regions, (e.g., Taniguchi et al. 2002). Other organisms with single burrows such as worms would be completely covered by seepage meters. These organisms would provide no net contribution of water to the seepage meter and may limit pumping water or completely cease pumping once the overlying water becomes anoxic. Single-burrow organisms surrounding the seepage meters would continue to pump water into and out of the sediment and thus could create pressure gradients through the sediment that would drive flow from outside to inside of the seepage meter.

*Chemical effects of exchange on  $^{222}\text{Rn}_{\text{excess}}$  activities*—Radioisotope tracers, particularly  $^{222}\text{Rn}$  and  $^{226}\text{Ra}$ , have become an important method for estimating the volumes of SGD (Cable et al. 1996a,b; Burnett et al. 2003). In one formulation of this technique, all sources and sinks of the tracers except for SGD are measured or calculated for a water column, and the mass balance for the water column is resolved by assuming that discrepancies result from advective flux of  $^{222}\text{Rn}$ - or  $^{226}\text{Ra}$ -rich groundwater (Cable et al. 1996a). Sources and sinks of  $^{222}\text{Rn}$  in the water column include in situ production and decay, horizontal transport, atmospheric evasion, and benthic exchange, which may be subdivided into pore water advection or diffusion, and groundwater sources. Rapid exchange of marine-derived pore water across the sediment–water interface could influence such mass balance calculations by contributing greater amounts of radioisotopes than would originate from diffusion or terrestrial groundwater fluxes.

The  $^{222}\text{Rn}_{\text{excess}}$  activity profiles in pore waters at CIRL39 increase steadily with depth, reflecting a source of Rn in the sediments (Fig. 3). Because the  $\text{Cl}^-$  concentrations indicate limited influx of freshwater at this site, the source of the  $^{222}\text{Rn}$  is assumed to be from radioactive decay of sediment-bound  $^{226}\text{Ra}$ . The sediment slurry experiments show  $^{226}\text{Ra}$  activities of  $\sim 9, 16, 23,$  and  $8 \text{ dpm L}^{-1}$  for sediments at depths of 28, 78, 110, and 158 cmbsf, respectively, with an increase in the activity to  $\sim 790 \text{ dpm L}^{-1}$  at 190 cmbsf. Along with this source of  $^{222}\text{Rn}$  to the pore waters, the shape of the  $^{222}\text{Rn}_{\text{excess}}$  profiles of the pore water also results from the low activity of  $^{222}\text{Rn}$  in the water column due to loss of Rn to the atmosphere (Fig. 3). Although a strong diffusional gradient develops between the  $^{222}\text{Rn}$ -poor surface water and the  $^{226}\text{Ra}$ -rich sediments at

190 cmbsf, the inflection in  $^{222}\text{Rn}_{\text{excess}}$  activity around 50 cmbsf (Fig. 3) shows that diffusion is not the only control of the shape of the profiles. Comparing the shape of the  $\text{Cl}^-$  concentration profiles with those of  $^{222}\text{Rn}_{\text{excess}}$  indicates that the inflection is caused by exchange of  $^{222}\text{Rn}$ -poor lagoon water with low  $^{222}\text{Rn}_{\text{excess}}$  activities in the water column.

Unlike  $\text{Cl}^-$  profiles, which have nearly identical concentrations between lagoon water and shallow pore waters, all  $^{222}\text{Rn}_{\text{excess}}$  activities in the mixed zone, except for the uppermost sample, are elevated above the values in the lagoon water, although less than the elevation in  $^{222}\text{Rn}$  activities at depths below 50 cmbsf (Fig. 3). These elevated activities are a product of at least two coupled mechanisms: production of  $^{222}\text{Rn}$  in the sediments by  $^{226}\text{Ra}$  and an enhanced upward mixing of  $^{222}\text{Rn}_{\text{excess}}$  from the  $^{226}\text{Ra}$ -enriched sediment zone at 190 cmbsf. This extra flux of  $^{222}\text{Rn}_{\text{excess}}$  would contribute to the  $^{222}\text{Rn}$  inventory in the lagoon water column, and if attributed to discharge from terrestrial aquifers, could lead to overestimates of the terrestrial groundwater discharge rate calculated from mass balance models of water column  $^{222}\text{Rn}$ .

*Chemical effects of exchange on nutrient fluxes*—Exchange across the sediment–water interface may enhance remineralization of organic carbon because of the flux of oxygen carried with the water during exchange. Although we have no precise measurements (e.g., Winkler titrations) of oxygen concentrations in the pore water, when we used field equipment to measure oxygen concentrations in the lagoon water, they were near saturation at  $\sim 0.4 \text{ mmol L}^{-1}$ . Measured oxygen concentrations in the pore waters are typically much less than 10% of this value. It is possible that pore-water oxygen concentrations could be even lower than measured if the water samples are contaminated with atmospheric oxygen during sampling from the open sampling containers.

As lagoon water exchanges with underlying pore waters, 100 mmoles oxygen per  $\text{m}^2 \text{ d}^{-1}$  would be reduced, using the more conservative estimate of volume of water exchanged across the sediment–water interface of  $0.2 \text{ m}^3 \text{ m}^{-2} \text{ day}^{-1}$  and assuming an average oxygen concentration of  $0.4 \text{ mmol L}^{-1}$  in the lagoon water. Assuming the reduction of this oxygen remineralizes organic matter with the Redfield ratio for carbon, nitrogen (N), and phosphorus, the oxygen flux to the sediments could generate N fluxes of  $\sim 10 \text{ mmol m}^{-2} \text{ d}$ , or  $3 \times 10^9 \text{ mol yr}^{-1}$  over the entire  $761 \text{ km}^2$  Indian River Lagoon. This flux calculation assumes conservative transport will occur for the remineralized N to the lagoon water. This estimated flux would not represent a new source of N to the system, however, and instead represents internal cycling of N to and from the water column.

These calculated fluxes must represent a maximum N flux from this source because some unknown amount of oxygen would be reduced during oxidation of sulfide, ammonia, iron, manganese, and other reduced chemical species dissolved in the pore water and in the sediment. Similarly, any denitrification that occurs would reduce the flux value because of retention of ammonium in the solid

phases. This estimated flux of N into the lagoon is an order of magnitude greater than estimated N fluxes of  $1.8 \text{ to } 4.0 \times 10^8 \text{ mol yr}^{-1}$  from rivers (Castro et al. 2001) and two orders of magnitude greater than estimated atmospheric deposition of  $1.4 \text{ to } 2.6 \times 10^7 \text{ mol yr}^{-1}$  (Dreschel et al. 1990; Castro et al. 2001). Unlike the flux associated with exchange across the sediment–water interface, nitrogen derived from rivers and atmosphere would represent a new source of N to the lagoon system. Other redox sensitive elements such as carbon, phosphorous, and metals are also likely to be influenced by the flux of oxygen-saturated surface water through shallow sediments.

In the Indian River Lagoon, measurements of chemical and thermal variations in shallow pore water demonstrate that water rapidly exchanges across the sediment–water interface. This exchange could explain the large discrepancies between SGD measured directly with seepage meters and radioisotopes, and numerical model estimates of the volumes of water that are available to discharge from terrestrial aquifers previously observed in other estuaries. The high rate of exchange also suggests the marine fraction of SGD is volumetrically more important than the terrestrial fraction, although the relative proportions of these two sources of water remain to be determined.

The exchange in this lagoon is driven largely by bioirrigating organisms because other processes, such as wave and tidal pumping, are minor in the region. Density inversion can occur between the lagoon and pore water, which would induce free convection. Nonetheless, in the summer, the densities of the lagoon and pore water are stably stratified, yet exchange is observed in chemical and thermal variations of the pore water. Burrowing organisms are common throughout the lagoon, and the published rates at which they exchange water are similar to the discharge rates measured using seepage meters. Similar effects from bioirrigation are likely in other estuaries and coastal settings wherever burrowing organisms occur, but may be masked if other processes, such as tidal and wave pumping, are extensive.

The water exchange is important for chemical fluxes from the sediment. The exchange enhances the flux of  $^{222}\text{Rn}$  from  $^{226}\text{Ra}$ -rich zones in the sediment and could be an important contribution of  $^{222}\text{Rn}$  to the water column along with discharge from terrestrial aquifers. This needs to be considered in mass balance models using  $^{222}\text{Rn}$  as a natural tracer. The exchange of water across the sediment–water interface could also recycle mass from the sediment through redox reactions with organic matter and metals associated with the sediment. Because nutrients originate from the detrital organic carbon, its ultimate source would be from the lagoon water and thus would not be considered a flux of new nutrients to estuary water.

## References

- ALLER, R. C. 1980. Quantifying solute distributions in the bioturbated zone of marine sediments by defining an average micro-environment. *Geochim. Cosmochim. Acta* **44**: 1955–1965.

- BOKUNIEWICZ, H., M. POLLOCK, J. BLUM, AND R. WILSON. 2004. Submarine ground water discharge and salt penetration across the sea floor. *Ground Water* **42**: 983–989.
- BOUDREAU, B. P., AND R. L. MARINELLI. 1994. A modelling study of discontinuous biological irrigation. *J. Mar. Res.* **52**: 947–968.
- BURNETT, W. C., H. BOKUNIEWICZ, M. HUETTEL, W. S. MOORE, AND M. TANIGUCHI. 2003. Groundwater and pore water inputs to the coastal zone. *Biogeochem.* **66**: 3–33.
- CABLE, J. E., G. C. BUGNA, W. C. BURNETT, AND J. P. CHANTON. 1996a. Application of  $^{222}\text{Rn}$  and  $\text{CH}_4$  for assessment of ground water discharge to the coastal ocean. *Limnol. Oceanogr.* **41**: 1347–1353.
- , W. C. BURNETT, J. P. CHANTON, AND G. L. WEATHERLY. 1996b. Estimating groundwater discharge into the northeastern Gulf of Mexico using radon-222. *Earth Planet. Sci. Lett.* **144**: 591–604.
- , P. W. SWARZENSKI, M. LINDENBURG, AND J. STEWARD. 2004. Comparative analysis of field and geochemical techniques for quantifying ground water discharge to coastal waters. *Ground Water* **42**: 1011–1020.
- CARSLAW, H. S., AND J. C. JAEGER. 1959. *Conduction of heat in solids*. Oxford Univ. Press.
- CASTRO, M. S., AND OTHERS. 2001. Contribution of atmospheric deposition to the total nitrogen loads to thirty-four estuaries on the Atlantic and Gulf coasts of the United States, p. 77–106. *In* R. A. Valigura, R. B. Alexander, M. S. Castro, T. P. Meyers, H. W. Paerl, P. E. Stacey, and R. E. Turner [eds.], *Coastal and estuarine studies*. American Geophysical Union.
- COOPER, J. H. H. 1959. A hypothesis concerning the dynamic balance of fresh water and salt water in a coastal aquifer. *J. Geophys. Res.* **64**: 461–467.
- DALES, P. R., C. P. MANGUM, AND J. C. TICHY. 1970. Effects of changes in oxygen and carbon dioxide concentrations on ventilation rhythms in onuphid polychaetes. *J. Mar. Biol. Assoc. UK* **50**: 365–380.
- DRESCHEL, T. W., B. C. MADSEN, L. A. MAULL, C. R. HINKLE, AND W. M. I. KNOTT. 1990. Precipitation chemistry: Atmospheric loadings to the surface waters of the Indian River Lagoon Basin by rainfall. *Environ. Chem.* **53**: 184–188.
- FORSTER, S., AND G. GRAF. 1995. Impact of irrigation on oxygen flux into the sediment—Intermittent pumping by *Callianassa subterranea* and piston pumping by *Lanice conchilega*. *Mar. Biol.* **123**: 335–346.
- HUETTEL, M., AND I. T. WEBSTER. 2001. Porewater flow in permeable sediments, p. 144–179. *In* B. P. Boudreau, and B. B. Jorgensen [eds.], *The benthic boundary layer transport processes and biogeochemistry*. Oxford Univ. Press.
- LEE, D. R. 1977. A device for measuring seepage flux in lakes and estuaries. *Limnol. Oceanogr.* **22**: 140–147.
- LI, H., AND J. J. JIAO. 2003. Tide-induced ground water fluctuations in a coastal leaky confined aquifer system extending under the sea. *Water Resour. Res.* **37**: 1165–1171.
- LI, L., D. A. BARRY, F. STAGNITTI, AND J.-Y. PARLANGE. 1999. Submarine groundwater discharge and associated chemical input to a coastal sea. *Water Resour. Res.* **35**: 3253–3259.
- LOUDEN, K. E., AND J. A. WRIGHT. 2000. Marine heat flow data: A new compilation of observations and brief review of its analysis, p. 3–27. *In* J. A. Wright, and K. E. Louden [eds.], *CRC handbook of seafloor heat flow*. CRC Press.
- MARTIN, J. B., J. E. CABLE, AND J. JAEGER. 2005a. Quantification of advective benthic processes contributing nitrogen and phosphorus to surface waters of the Indian River Lagoon. St. Johns River Water Management District. p. 244.
- , ———, ———, M. ROY, K. HARTL, AND C. G. SMITH. 2005b. Separating marine and terrestrial submarine ground water discharge. Geological Society of America, Annual Meeting, Salt Lake City, Utah.
- , P. W. SWARZENSKI, AND M. K. LINDENBERG. 2004. Mixing of ground and estuary waters: Influences on ground water discharge and contaminant transport. *Ground Water* **42**: 1000–1010.
- , K. M. HARTL, D. R. CORBETT, P. W. SWARZENSKI, AND J. E. CABLE. 2003. A multilevel pore water sampler for permeable sediments. *J. Sediment. Res.* **73**: 128–132.
- MICHAEL, H. A., A. E. MULLIGAN, AND C. F. HARVEY. 2005. Seasonal oscillations in water exchange between aquifers and the coastal ocean. *Nature* **436**: 1145–1148.
- MILLER, D. C., AND W. J. ULLMAN. 2004. Ecological consequences of ground water discharge to Delaware Bay, United States. *Ground Water* **42**: 959–970.
- MOORE, W. S. 1996. Large groundwater inputs into coastal waters as revealed by  $^{226}\text{Ra}$  enrichment. *Nature* **380**: 612–614.
- , AND A. M. WILSON. 2005. Advective flow through the upper continental shelf driven by storms, buoyancy, and submarine groundwater discharge. *Earth Planet. Sci. Letters* **235**: 564–576.
- RIISGARD, H. U., I. BERNTSEN, AND B. TARP. 1996. The lugworm (*Arenicola marina*) pump: Characteristics, modelling and energy cost. *Mar. Ecol. Prog. Ser.* **138**: 149–156.
- SCHLUTER, M., E. SAUTER, H.-P. HANSEN, AND E. SUESS. 2000. Seasonal variations of bioirrigation in coastal sediments: Modelling of field data. *Geochim. Cosmochim. Acta* **64**: 821–834.
- SHINN, E. A., C. D. REICH, AND T. D. HICKEY. 2002. Seepage meters and Bernoulli's revenge. *Estuaries* **25**: 126–132.
- SHUM, K. T. 1993. The effects of wave-induced pore water circulation on the transport of reactive solutes below a rippled sediment bed. *J. Geophys. Res.* **98**: 10,289–10,301.
- SMITH, N. P. 1993. Tidal and nontidal flushing of Florida's Indian River Lagoon. *Estuaries* **16**: 739–746.
- TANIGUCHI, M., W. C. BURNETT, J. E. CABLE, AND J. V. TURNER. 2002. Investigations of submarine groundwater discharge. *Hydrol. Process.* **16**: 2115–2129.
- TIMMERMANN, K., J. H. CHRISTENSEN, AND G. T. BANTA. 2002. Modeling of advective solute transport in sandy sediments inhabited by the lugworm *Arenicola marina*. *J. Mar. Res.* **60**: 151–169.
- WEBB, A. P., AND B. D. EYRE. 2004. Effect of natural populations of burrowing thalassinidean shrimp on sediment irrigation, benthic metabolism, nutrient fluxes and denitrification. *Mar. Ecol. Prog. Ser.* **268**: 205–220.

Received: 12 August 2005

Amended: 18 December 2005

Accepted: 9 January 2006